



Dependence of pH and temperature effect in the synthesis of Fe₃O₄

M.Gurumoorthy*, M. Anbarasu, K.Parasuraman, K.Balamurugan

Department of Physics, Poompuhar College (Autonomous), Melaiyur, Tamil Nadu, India

Department of Physics, Annamalai University, Chidambaram, Tamil Nadu, India

Abstract : Fe₃O₄ nanoparticles were synthesized via chemical co-precipitation method using Hexamethylenediamine (C₆H₁₆N₂) as a precipitating agent and a base. It was found that the value of pH and temperature influences the reaction mechanism for the formation of Fe₃O₄ nanoparticles. The obtained nanoparticles was characterized by X-ray diffraction (XRD), Fourier transform infrared spectrometer (FT-IR), Field emission scanning electron microscopy (FE-SEM), Field emission transmission electron microscopy (FE-TEM) and thermo gravimetric analysis (TGA), their magnetic study was analysis by vibrating sample magnetometer.

Keywords. Fe₃O₄ nanoparticles, pH and temperature, co-precipitation.

Introduction

Magnetite (Fe₃O₄), has attracted considerable interest because of its remarkable properties, which recommended it for a wide field of applications, such as: ferrofluids, magnetic hyperthermia, magnetic resonance imaging (MRI), magnetic drug delivery, catalyst, magnetic storage media, removal of different containments from water, etc¹⁻⁶. However magnetic nanoparticles are the most studied materials due to their response to magnetic field through the superparamagnetic behavior at room temperature with high saturation magnetization, in addition, their non-toxicity and high biocompatibility are also suitable for biotechnology areas⁷. The particle size is the main factor that effects many interesting properties, for example, a particle size in the nanometer range can pass through a capillary vessel to bind with a protein or DNA, whereas, a micrometer particle will react with cells only^{8,9}. Moreover, the critical size should be in the range of 30-50nm in order to achieve the single domain particles and the superparamagnetic behavior¹⁰. At the same time, the production of pure Fe₃O₄ powders with appropriate features (large surface area, small particle size, narrow size distribution, good magnetic properties etc.) has always been a challenge¹¹. Therefore several synthesis methods have been suggested: sol-gel¹², hydrothermal¹³, thermal decomposition of different precursors¹⁴⁻¹⁷, spray pyrolysis¹⁸, carbothermal reduction¹⁹, co-precipitation method²⁰, etc. For example, the chemical co-precipitation provides spherical shape with particle size below 25nm²¹.

In this work we were able to improve the co-precipitation procedure, through which the exact dependence of pH and temperature on the synthesis of Fe₃O₄ were studied elaborately.

Experimental

Synthesis of Fe₃O₄ nanoparticles

Materials

For the present investigation, Fe₃O₄ magnetic nanoparticles are chosen to be the principle component. For synthesis Analytical Reagent grade chemicals were used without further purification. Highly purified water is used for all dilution process and sample preparation. All the chemicals namely Ferrous chloride, ferric chloride, *hexamethylenediamine*, acetone and methanol were purchased from Sigma Aldrich which has 98% purity. For the present investigation, Fe₃O₄ magnetic nanoparticles are chosen to be the principle component.

Co-precipitation Process

Co-precipitation is a facile and convenient way to synthesize iron oxides (either Fe₃O₄ or γ -Fe₂O₃) from aqueous Fe²⁺/Fe³⁺ salt solutions by the addition of a base under inert atmosphere at room temperature or at elevated temperatures. The size, shape, and composition of the magnetic nanoparticles very much depends on the type of salts used (e.g. chlorides, sulfates, nitrates), the Fe²⁺/Fe³⁺ ratio, the reaction temperature, the pH value and ionic strength of the media. With this synthesis, once the synthetic conditions are fixed, the quality of the magnetite nanoparticle is fully reproducible. The magnetic saturation values of magnetite nanoparticles are experimentally determined to be in the range of 30-50 emu/g, which is lower than the bulk value, 90 emu/g so chemical co-precipitation method was selected to carry out the synthesis.

Mechanism

The mechanism of the formation of Fe₃O₄ nanoparticles with ferrous and ferric salts at the ratio of 1:2, by the 'co-precipitation' method is represented by the equation in which stoichiometric amounts of ferrous and ferric ions react to produce Fe₃O₄;



Synthesis Procedures

The variation of pH has significant effect in nanoparticles synthesization. So it is essential to find the optimum pH values of the solution from which the nanoparticles are synthesized. To investigate the same, the Fe₃O₄ nanoparticles were synthesized from the solution with different pH values using the procedure as follows.

Ferric chloride (0.033M) and ferrous chloride (0.017M) were mixed in 100 ml water. Hexamethylenediamine (0.25M) was added in drop so as to obtain the solution of pH 11.5. The solution was continuously stirred using a magnetic stirrer for three hours for the completion of nucleation process. The final product was washed 3 times with methanol and distilled water. The precipitate was separated using centrifugation and washed to remove excess water contained in it. The final precipitate was dried in hot air oven at 60°C to get the product. The same procedure is repeated to obtain nanoparticles from the solution with different pH values, by changing the quantity of the Hexamethylenediamine. The names of the samples with their respective pH values were tabulated (Table 1).

Table 1. pH effect in the synthesis of Fe₃O₄ nanoparticles

Sample names	pH values	Hexamethylenediamine Mole concentration (M)
S ₁	11.5	0.25
S ₂	10	0.20
S ₃	9	0.15
S ₄	8.5	0.10
S ₅	7.2	0.05

Variation of temperature has direct impact on the dispersibility and saturation magnetization of the nanoparticles, hence the study of the effect of temperature is inevitable in nanoparticles synthesis. In the present work Fe₃O₄ nanoparticles have been synthesized using chemical co-precipitation method at four different temperatures from 37°C to 80°C in order to study the temperature effect, and are tabulated in (Table 2).

Table 2. Temperature effect in the synthesis of Fe₃O₄ nanoparticles

Sample names	Temperature(°C)
S ₁	RT (37)
T ₁	40
T ₂	60
T ₃	80

Characterizations

Fe₃O₄ nanoparticles were characterized using various analysis techniques namely XRD, FT-IR, FE-SEM, FE-TEM, TGA and VSM. The elemental composition of the nano materials were estimated using SEM. Morphological information on the nanoparticles was obtained using SEM and FE-TEM. The crystalline phase and crystal structure were analyzed using XRD and FE-TEM. Different functional group and their changes were analyzed using FT-IR, TGA are chose to analyze the thermal behavior of nano materials and the magnetic characterization was carried out using VSM.

Result and Discussion

The effect of pH

XRD Measurement was conducted to identify the sample phase in varying pH. (Figure 1) the XRD pattern of sample a, b and c with pH values of 11.5, 10 and 9, the Fe₃O₄ phase was identified in sample a, b and c, all of the peaks were matching with standard file of Fe₃O₄ (JCPDS#19-029). While three peaks positioned at $2\theta = 30.13^\circ$, 35.48° , 43.12° and 62.81° can be assigned to the (220), (311), (400) and (440) planes, respectively, which indicates the cubic spinel crystal structure of pure Fe₃O₄. (Figure 2) show the XRD pattern of sample d with pH value of 8.5, the hematite (α -Fe₂O₃) phase was identified with standard file of α -Fe₂O₃ (JCPDS#1309-1) expect two peaks positioned at $2\theta = 36.01^\circ$ and 46.98° which are (310) and (330) planes. (Figure 3) show the XRD pattern of sample e with the pH of 7.23, the maghemite (γ -Fe₂O₃) phase was identified with standard file of γ -Fe₂O₃ (JCPDS#25-1402), while three peaks positioned at $2\theta = 16.83^\circ$, 24.3° , and 64.6° . Moreover, the average crystallite size can be estimated by X-ray diffraction pattern, using the scherrer,s equation ²²:

$$\beta = \frac{K\lambda}{d \cos \theta}$$

where, β is the peak width at half of maximum intensity, K is the shape factor, λ is the X-ray diffraction wavelength ($\lambda = 0.154$ nm), d is the average crystallite size and θ is the bragg angle in degree, it should be noted that the shape factor K is rotated with several factors, indicating the miller index of the reflection plane and the shape of the crystal, is normally 0.89 ²³. The result, listed in Table 3. Show, in the all entire XRD results, the sample a with pH level of 11.5 is the better crystallinity and also Fe₃O₄ phase is obtained.

Figure 1. XRD patterns of sample a, b and c

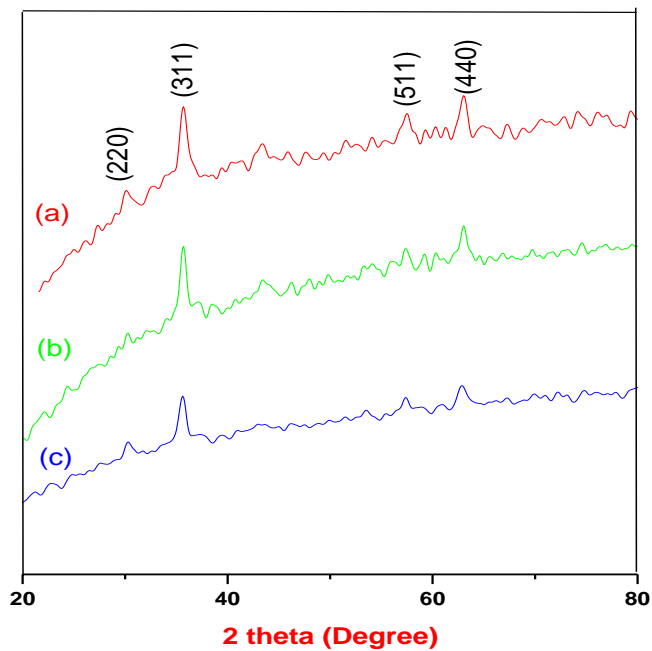


Figure 2. XRD pattern of sample d

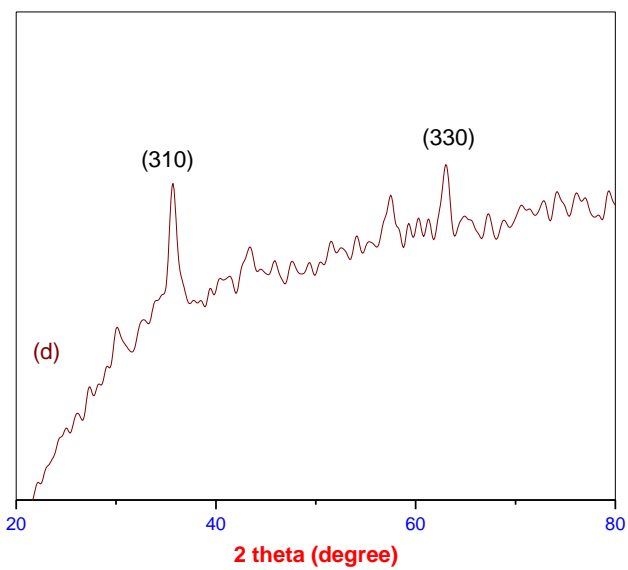


Figure 3. XRD pattern of sample e

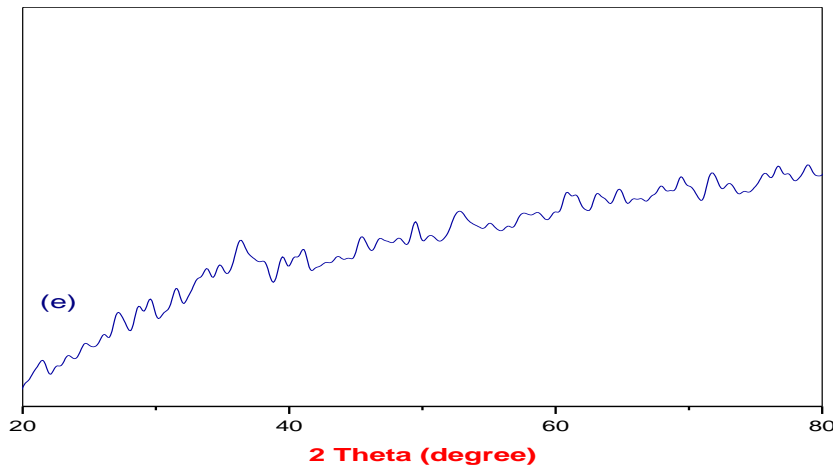


Table 3. List of the pH values, 2θ, Chemical phase and particle sizes of the samples.

Sample	pH values	2θ values	Chemical phase	Particle size(nm)
A	11.5	35.4	Fe ₃ O ₄	12.8
B	10	35.5	Fe ₃ O ₄	10.3
C	9	35.6	Fe ₃ O ₄	10.1
D	8.5	36.0	α-Fe ₃ O ₄	8.3
E	7.2	16.9	γ-Fe ₃ O ₄	8

The effect of reaction temperature (T)

(Figure 4) the XRD pattern of sample A, T₁, T₂ and T₃ revealed that the Fe₃O₄ phase was identified from sample A and T₁, all of the peaks were matching standard file of Fe₃O₄ (JCPDS#19-029). While four peaks positioned at 2θ = 30.13°, 35.48°, 43.12° and 62.81° can be assigned to the (220), (311), (400) and (440) planes, respectively, which indicates the cubic spinel crystal structure of pure Fe₃O₄. Fig.4.4 shows the XRD pattern of sample T₂ and T₃ revealed that, the hematite (α-Fe₂O₃) phase was identified with standard file of α-Fe₂O₃ (JCPDS#1309-1) expect two peaks positioned at 2θ = 36.01° and 46.98° which are (310) and (330) planes moreover, their crystalline size were listed in (Table 4).

Figure 4. X-ray diffraction pattern of samples A, T₁, T₂ and T₃

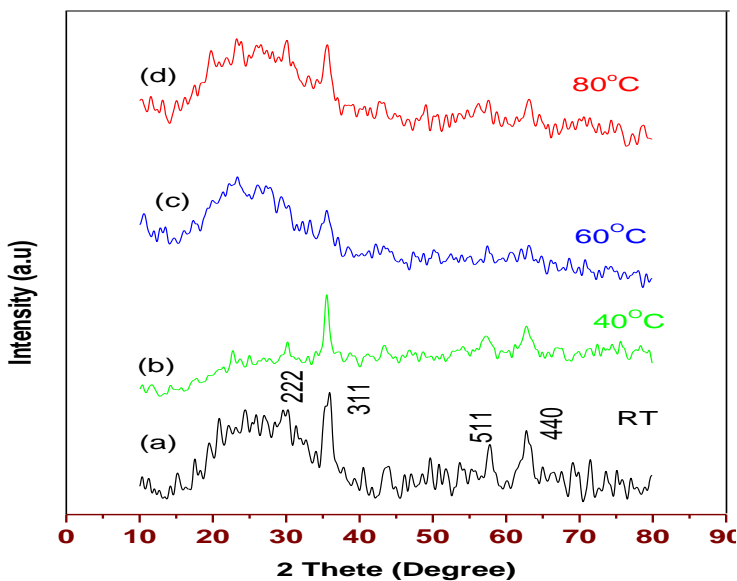


Table 4. List of the pH values, 2θ , Chemical phase and particle sizes of the samples

Sample	Temperature ($^{\circ}\text{C}$)	2θ values	Chemical phase	Particle size(nm)
A	37	35.60	Fe_3O_4	8.56
T ₁	40	35.20	Fe_3O_4	14
T ₂	60	36.01	$\alpha\text{-Fe}_2\text{O}_3$	8.26
T ₃	80	36.00	$\alpha\text{-Fe}_2\text{O}_3$	278

The FT-IR spectrum of the Fe_3O_4 (sample a with pH level of 11.5) nanoparticles are shown in (Figure 5). Three absorption peaks are visible the absorption peak at 3421 cm^{-1} corresponds to surface of OH stretching vibrations²⁴. The two distinct absorption peaks at 571 and 430 cm^{-1} are attributed to the vibration of $\text{Fe}^{2+} - \text{O}^{2-}$ and $\text{Fe}^{3+} - \text{O}^{2-}$, respectively²⁵. The absorption bands between 450 and 700 cm^{-1} are probably also due to lattice vibrations of Fe-O bonds in iron oxide. Therefore as claimed with previous researcher sharp and highly intense peak appeared at 571 cm^{-1} demonstrates a high degree of crystallinity of Fe_3O_4 NPs^{24, 26, 27}.

(Figure 6) shows the FE-SEM image (a), FE-TEM image (b and c) and SAED pattern (d) of Fe_3O_4 nanoparticles (sample A with the pH level of 11.5), as shown in (Figure 6 b and c), the nanoparticles have average size of 15 nm with narrow size distribution which is in consistent with the estimation from XRD results ($d_{\text{XRD}}=13\text{ nm}$). It should be noted that the obtained Fe_3O_4 nanoparticles possess well-defined and homogeneous shape, as shown in (Figure 6 d), the Selected area electron diffraction pattern (SAED) reveals that the sample is satisfactory polycrystalline of cubic spinel crystal structure, which is in accordance with the XRD result. FE-SEM image, as shown in (Figure 6 a), presents the morphology of the Fe_3O_4 nanoparticles is roughly spherical shape, it has been reported that spherical shape is formed because the nucleation rate per unit area is isotropic at the interface between the Fe_3O_4 magnetic nanoparticles^{28, 29}.

TG analysis was carried out to know the temperature at which the precursor is completely converted into the desired metal oxide. The curve obtained from the TG analysis is shown in (Figure 7), from which, it is evident that the decomposition of the precursor starts at around 85°C and at 475°C it shows 4.5% residue, indicating the formation of Fe_3O_4 . The weight loss curve becomes linear after 475°C , signifying no further changes in composition of the material.

The magnetic properties of Fe_3O_4 (sample a with pH level of 11.5) nanoparticles were measured out at room temperature using vibrating sample magnetometer, as shown in (Figure 8), it can be seen that the magnetization curves appear s-shaped over the applied magnetic field and the samples exhibit typical super paramagnetic behavior, showing zero coercivity, which means that they are attributed by an external magnetic field but retain no residual magnetism which the external magnetic field is removed at room temperature. The saturation magnetization (M_s) of the Fe_3O_4 nanoparticles is 62 emu/g , it has been reported that M_s of $7\text{-}22\text{ emu/g}$ is adoptable for biomedical application³⁰. Therefore, the level of saturation magnetization(M_s) achieved for Fe_3O_4 nanoparticles are promising for MRI contrast agent. The inset in Fig. 4.8 shows the efficient magnetic separation process in a short time (about 30 s), which was very favorable for the magnetic separation of toxic pollutants from extreme environments in practical engineering aspect.

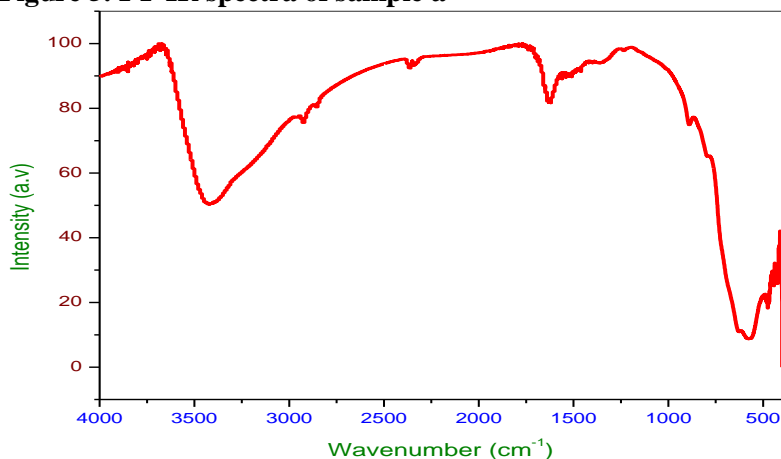
Figure 5. FT-IR spectra of sample a

Figure 6. FE-SEM image (a), FE-TEM images (b and c) and SAED pattern (d) of sample a

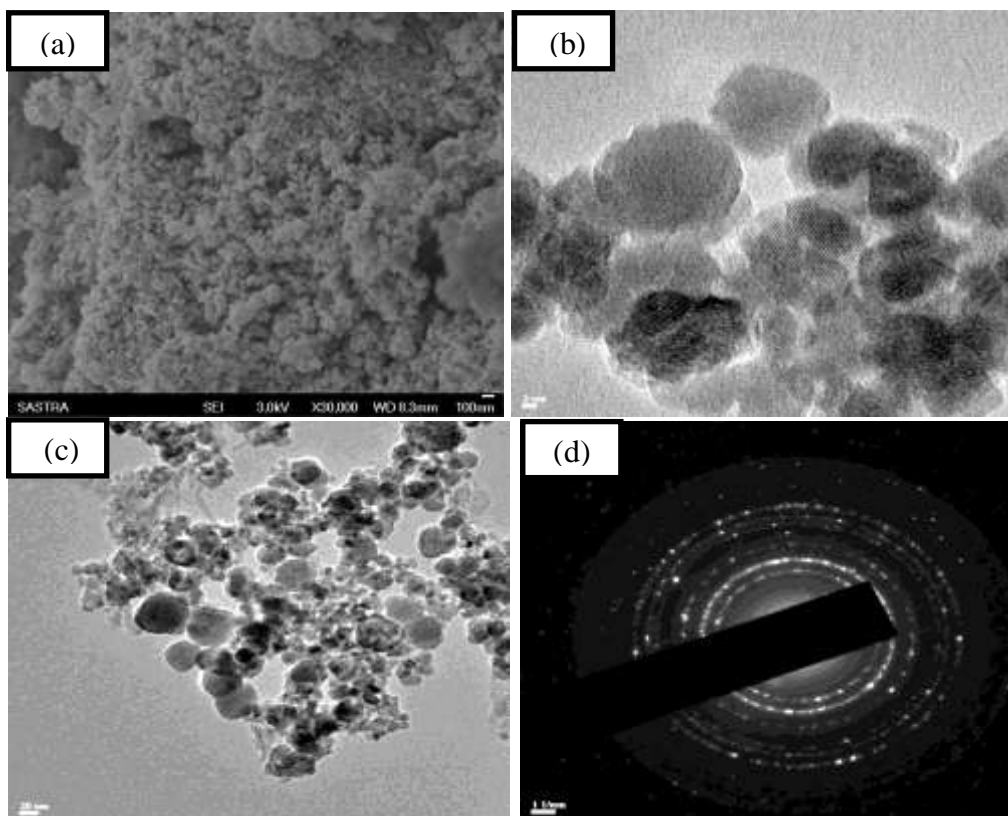


Figure 7. DGA analysis of sample a

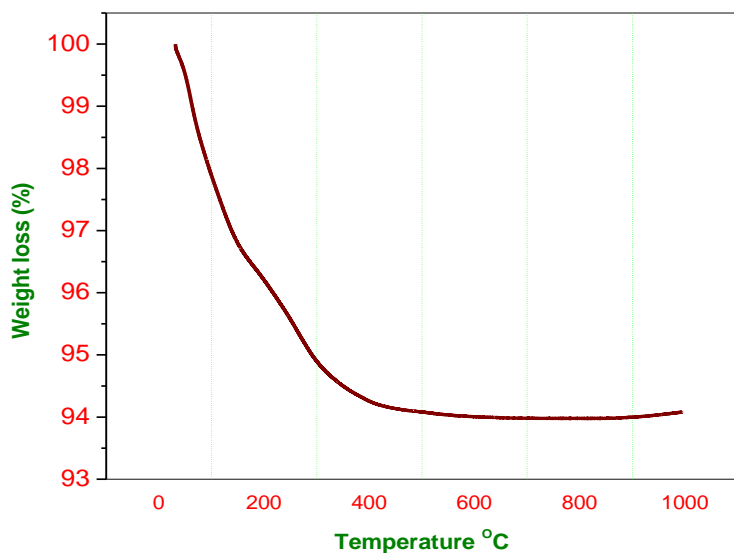
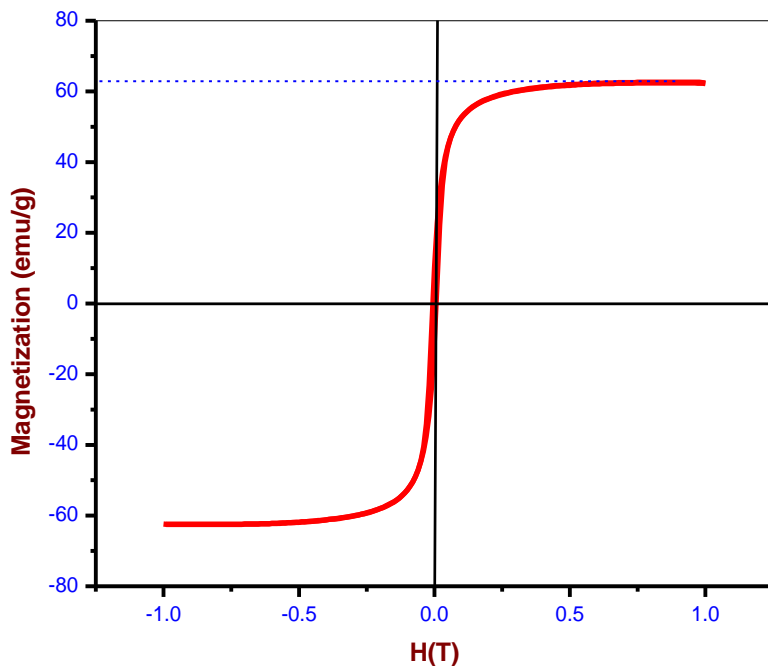


Figure 8. Magnetization curves of sample a



Conclusion

The method of synthesis of Fe₃O₄ nanoparticles by chemical co-precipitation method was investigated with a focus on the dependence of pH on the formation of Fe₃O₄ nanoparticles. It is verified that the value of pH has a major role in the formation of Fe₃O₄ phase XRD reveals that the as-synthesized nanoparticles α-Fe₂O₃ or Fe₃O₄ with an average diameter of 13 to 8nm. The Fe₃O₄ nanoparticles with optimized shape and magnetic properties, synthesized by controlling the pH in the solution containing ferrous and ferric ions can be applied in biological and biomedical fields, especially, the high saturation magnetization of Fe₃O₄ is a very convenient to magnetic resonance imaging (MRI) contrast agent.

References

1. S. R. Dave and X.Gao, *Nanomed. Nanobiotechnol.* 1 , 2011 , 583-609
2. N. Stepova and O. Kushka, *Chem. Chem. Technol.*, 5 , 2011, 155-160.
3. T. E. Babutina, N. V. Boshitska, O. A. Ivashchenko, A. O. perekosn, V. Z. Voinash and I. V. Uvarova, *Powder Metall. Met. Ceram.*, 48 , 2009, 365-370.
4. L.vekas., *Adv. Sci. Tech.*, 54 , 2008 , 127-136.
5. Asuha, B. Suyala, and S. Zhao, *Mater. Chem. Ohys.*, 129 , 2011, 483-487.
6. J. T. Mayo, C. Yavuz, S.yean, L. Cong, H. Shipley, W. Yu, J. Falkner, A.Kan, M. Tomson, and V. L. Colvin, *Sci. Technol. Adv. Mater.*, 8 , 2007, 71-75.
7. P.Lamor, B. S. Inbaraj, B. H. Chen, *Mater. Scie. Engi. B* 45 , 2010, 1603-1607.
8. A. Iida, K. Takayanagi, T. Nakanishi, T.Osaka, *J. Colloid interface Sci.*, 314 , 2007, 274-280.
9. M. Arnebo, R. F. Pacheco, M. R. Ibarra, J. Santamarra, *Nanotoday.*, 2 , 2007, 22-32
10. J. Murbe, A. Rechtenbach, J. Topfner, *Mater. Chem.. phys.* 110 , 2008, 426-433
11. T. K. Indira, *Int. J. Pharm. Sci. Nanotech.* 3 , 2010, 1035-1042.
12. J.Xu, H.Yang, W. Fu, K.Du, Y. Sui, J. Chen, Y. Zang, M. Li, G. Zou, *J. Magn. Magn. Mater.* 309 , 2007, 307-3011.
13. S. Liu, F. Lu, R. Xing, J. Zhu, *Chem. Eur. J.* 17 , 2011, 620-625.
14. S. Asuha, B. Suyala, X. Sigintra, S.Zhao, *J. Alloys. Compd.* 43 , 2002, 2179-2184.
15. J. Toper, A. Angermann, *Marer. Chem. Phy.* 129 , 2011, 337-342.
16. L. Chen, Z. Liu, C. Zhao, Y. Zhang, Y. Zhou, H. Peng, *J. Alloy. Compd.* 509 , 2011, 11-15

17. X. Liu, Y. Guo, Y. Wang, J. Ren, Y. Wang, Y. Guo, G. Lu, Y. Wang, J. Ren, Y. Wang, Z. Zhang. *J. Mater. Sci.* 45 , 2010, 906-910.
18. R. Strobel, S. E. Pratsinis. *Adv. Powder. Tech.* 20 , 2009, 190-194
19. P. Hu, S. Zhang, H. Wang, D. Pan J. Tain, Z. Tag, A. A. Volinsky, *J. Alloys compound.*, 5 , 2011, 2316-2319
20. K. Petchavoen, A. Sirivat, *Mat. Scie. Engi.B* 177 , 2012, 421-427
21. X.Liu, M. D. Kaminski, Y. Guan, H. Chen, H. A. J. Lui, *J. Mag. Magn. Mater.*, 306 , 2006, 248-253.
22. W. S. Lu, Y. H. Shen, A.J. Xie, W. Q. Zhang, *J. Magn. Magn. Mater.* 322 , 2010,1828-1833.
23. D.K. Kim, M. Mikhaylova, Y. Zhang, M. Muhammed, *Chem. Mater.* 15 , 2003, 1617-1627.
24. S. Ahmod, U. Riaz, A. Kaushik, J. Alam. *J. Inorg. Organomet. Poly.* 19 , 2009, 355-360.
25. T. P. Z. Y. Zhong. I. Felner, A. Gedanker. *J. Phy. Chem b.* 103 , 1999, 947.
26. M. Qing, Y. Yang, B. wu, H. Wong, H. Wang, J. Xu, C. Zhang, H. X. Y. Li, *Catalysis Today* 185 , 2012, 79-87.
27. H. A. Khalaf. *Textural Monatshefte. Chemie* 140 , 2009, 669-674.
28. N.A. Brusentov, V.V. Gogosov, T. N. Brusentov, A.V. Sergeev, N.Y. Jurchenko, A.A Kuznetsov, O.A. Kuzenetsov, L.I. Shumakov, *J. Magn. Magn. Mater.* 225 , 2001, 113-117.
29. C.J. Xu, K.M. Xu, H.W. Gu, X.F. Zhong, Z.H. Guo, R.Zheng, X. Zhang, B. Xu, *J. Amer. Chem. Soc.* 126 , 2004, 3392-3401.
30. N.A. Brusentov, V.V. Gogosov, T. N. Brusentov, A.V. Sergeev, N.Y. Jurchenko, A.A Kuznetsov, O.A. Kuzenetsov, L.I. Shumakov, *J. Magn. Magn. Mater.* 225 , 2001, 113-117.
